Available online at www.sciencedirect.com
ScienceDirect
Mathematical Biosciences 209 (2007) 292–315
Mathematical Biosciences
www.elsevier.com/locate/mbs

Chemotherapy for tumors: An analysis of the dynamics and a study of quadratic and linear optimal controls ☆

L.G. de Pillis [a], W. Gu [a], K.R. Fister [b,*], T. Head [a], K. Maples [a], A. Murugan [a,c], T. Neal [b], K. Yoshida [a]

[a] *Department of Mathematics, Harvey Mudd College, Claremont, CA 91711, United States*
[b] *Department of Mathematics, Murray State University, Murray, KY 42071, United States*
[c] *Department of Mathematics, Pomona College, Claremont, CA 91711, United States*

Received 8 November 2005; received in revised form 13 April 2006; accepted 12 May 2006
Available online 26 May 2006

Abstract

We investigate a mathematical model of tumor–immune interactions with chemotherapy, and strategies for optimally administering treatment. In this paper we analyze the dynamics of this model, characterize the optimal controls related to drug therapy, and discuss numerical results of the optimal strategies. The form of the model allows us to test and compare various optimal control strategies, including a quadratic control, a linear control, and a state-constraint. We establish the existence of the optimal control, and solve for the control in both the quadratic and linear case. In the linear control case, we show that we cannot rule out the possibility of a singular control. An interesting aspect of this paper is that we provide a graphical representation of regions on which the singular control is optimal.

MSC: 49J15; 49K15; 92C50

Keywords: Chemotherapy; Singular; Bang–bang controls

☆ This work was supported by the National Science Foundation under Grant NSF-DMS-041-4011.
* Corresponding author. Tel.: +1 270 809 2491; fax: +1 270 809 2314.
E-mail addresses: depillis@hmc.edu (L.G. de Pillis), gu@hmc.edu (W. Gu), renee.fister@murraystate.edu (K.R. Fister).

0025-5564/$ - see front matter
doi:10.1016/j.mbs.2006.05.003

1. Introduction

In the context of mathematically modeling cancer growth with chemotherapy, it is common to frame an optimal control problem so that the total amount of drug is minimized, cf. [54,28]. This is done because of the *implicit* understanding that chemotherapy has damaging side effects. A weakening of the patient's immune system is one of the more dangerous side effects of many forms of chemotherapy, which can result in the patient becoming prone to infection, as well as diminishing the immune system's ability to help fight the cancer.

In the tumor growth model presented in this paper, we include an *explicit* representation of the immune system, as well as chemotherapy treatment. This allows us not only to incorporate the beneficial effects of the immune system on controlling the growing tumor, but also to track directly the detrimental effects of chemotherapy on both the tumor cell and the immune cell populations. It is common clinical practice to use the count of circulating lymphocytes in a patient's bloodstream as a reflection of the strength of the patient's overall immune health. Although it is understood that this does not provide a complete profile of the patient's immune health, it is accepted as one measure. Therefore, in this model we include two immune components: effector–immune cells and circulating lymphocytes. The effector–immune cells actively target and destroy tumor cells, while, as stated, the circulating lymphocytes serve as a way to monitor the additional damaging side-effects of chemotherapy.

Kuznetsov and Knott [44] have developed a deterministic model that describes the interplay of the cancer cells and the cytotoxic killer cells. Even though they have included only one immune cell population, they have described effectively the mechanisms of tumor growth, suppression, and regrowth using data on B-cell lymphoma in mice. Comparison to our results with optimal control techniques will be addressed. Work by Symanska [67] has recently included use of natural killer cells and lymphokine activated killer cells, in addition to cytotoxic T and B lymphocytes. Symanska uses the immune components as a vaccine, whereas we include effector–immune cells and circulating lymphocytes as naturally occurring cell populations that interact with the tumor cells. Symanska's work does not include Michaelis–Menton interaction terms in the effector–immune cell relationship with the tumor and she notes that her model could be improved with the inclusion of such to better reflect the cancer evolution. We have included Michaelis–Menton dynamics which reflect saturation-limited tumor growth.

The goal of this paper is to analyze and computationally explore two different optimal control strategies, one quadratic control and one linear control, on the coupled system of ordinary differential equations representing the above described tumor–immune-chemotherapy dynamics. Quadratic controls are generally more theoretically tractable, while linear controls, although they present some analytical challenges, are worth examining since they allow for the use of somewhat more intuitive objective functionals. This exploration of various control strategies may be considered as a first step toward the determination of theoretically improved approaches to treating a cancer patient. In both the quadratic and linear cases, we use Pontryagin's Maximum/Minimum Principle [60], which provides first order necessary conditions for a control to be optimal. In addition, the classical Clebsch condition [39] requires that the Hessian of the Hamiltonian, H, with respect to the control, u, must be non-negative definite, for this control to be minimizing. That is, $\frac{\partial^2 H}{\partial u^2} \geqslant 0$. This condition is trivially satisfied when all the controls occur linearly in the Hamiltonian, since the Hessian is identically zero. In this case, the possibility

of singular arcs arises and higher order necessary conditions are given by the Generalized Legendre Clebsch conditions [43].

A singular arc is an interval for which, given $n \geqslant 1$ control variables u_i, $i = 1, \ldots n$, one or more of the control variables satisfies

$$\frac{\partial H}{\partial u_i} = 0.$$

It can be shown that a singular control u_i will first appear only in an even order derivative of $\frac{\partial H}{\partial u_i}$ [43]. The order of the singularity of a control u_i, on this interval, is defined as the least integer q_i such that

$$\frac{\partial}{\partial u_i}\frac{\mathrm{d}^{2q_i}}{\mathrm{d}t^{2q_i}}\frac{\partial H}{\partial u_i} \neq 0.$$

See the Appendix for statements of the theorems related to the minimum principle and the necessary conditions for the Generalized Legendre Clebsch theory.

Recent studies have illustrated the effective use of the Generalized Legendre Clebsch condition in a general class of mathematical models of cancer chemotherapy [66]. In [66], three control strategies are analyzed. One is a killing agent which is active during cell division, another is a blocking agent which slows down cell growth, and a third is the recruitment of dormant tumor cells to enhance their efficient treatment by a cytotoxic drug. Within this study, the authors have found the singular controls are not optimal. In our work, we have introduced a model that involves a cytotoxic chemotherapeutic control that can directly and indirectly kill tumor cells and slow cell growth of tumor and immune cells, and have found regions in which the singular controls may be optimal. Ledzewicz et al. [47] provides insight into the use of quadratic and linear controls for a bilinear optimal control problem related to cancer chemotherapy. The form of the equations in [47] make the analytic computation of the Generalized Legendre Clebsch condition tractable. Also, in [48], the authors investigate drug resistance in a cancer chemotherapeutic optimal control model in which they include two killing agents that generate resistant populations. Within our work, the study of the interaction with the immune and tumor populations has mathematical similarities with their two compartment model of [48] involving gene amplification.

Other work in the intersection of optimal control and cancer therapy include Matveev and Savkin [54,28,27,16,17,9]. Each of these studies aims to reduce the tumor burden. The works by de Pillis and Radunskaya [16,17] focus on optimally controlling the application of chemotherapy to minimize total tumor while constraining the immune state to stay above a specified threshold. This model was shown to potentially have two stable attractors, so that a successful treatment strategy could drive the tumor population to stable undetectably small levels. The differences in these works originate in the dynamics of the models, use of state constraints, inclusion of stochastic components to the model, and the various objective functionals that one minimizes or maximizes. Each model provides qualitative strategies for control, but Coldman and Murray's model [9] is able to capture the data. The goal for our work is to develop qualitative results so that in future work we can project what will happen for real patient data.

Although the previous cited works had indirect connections to tumor–immune interactions, work by Kirschner and Panetta [41] led to optimal control problems directly involving immuno-

therapy. For example, in Burden et al., [5] and Fister and Donnelly [26], the model the model by Kirschner and Panetta was investigated with the inclusion of the controls in the form of adoptive cellular immunotherapy. The use of linear and quadratic controls was investigated and the numerics found that the controls could produce results that would reduce the tumor, but after a period of dormancy, the tumor cells would reappear. The resurgence was, however, at a level of magnitude lower than the previous occurrence. Yet, the Burden et al. and Fister and Donnelly papers were not able to graphically depict the region on which an optimal singular arc could exist. In the work that follows, we are able to provide this unique graphical depiction of the minimality of a singular arc for the optimal control drug regimen via numerical results.

2. Three-cell one-chemical model

In an increasing number of recently published mathematical models of tumor growth, some form of tumor–immune interaction is often included. In [15] and references one can find a detailed discussion of the importance of including an immune component in a cancer growth model, as well as a partial list of such tumor–immune mathematical models, which includes [2,3,7,8,20,13,11,42,12,14,19,25,30–33,35,40,46,49,52,56,57,63–65,68,70–72,74,75]. In [15] it is pointed out that the presence of an immune component in a mathematical model has been shown to be essential for producing clinically observed phenomena such as tumor dormancy, oscillations in tumor size, and spontaneous tumor regression. In addition, from a clinical perspective, the evidence for the potential of immune system control of certain malignancies has motivated new research into the development of immunotherapies and vaccine therapies for cancers. See, for example [4,10,22,58,61,73].

The model developed in this section also includes representations of immune system components, and provides a tractable testbed from which to explore the question of linear versus quadratic optimal control of chemotherapy in more detail. Future work may extend this model to include ways to apply immunotherapy so that the optimal control of combined chemo-immunotherapy may be investigated. Currently, the immune system components are present as a way to allow for natural immune interactions with the tumor, to observe the detrimental side-effects chemotherapy may have on a patient's immune system, and to monitor patient health.

The model we present tracks three cell populations and one drug concentration in the bloodstream. It is much like the model developed by de Pillis and Radunskaya [16], but differs in two respects. First, the model presented herein includes a circulating lymphocyte population as a measure of patient health, which replaces the 'normal cell' population used in [16]. Second, in order to simplify the optimal control analysis, the dose–response dynamics are represented by mass-action terms instead of exponentially decaying terms.

The cell populations and drug concentration in this model at time t are denoted by:

- $T(t)$, tumor cell population
- $N(t)$, effector–immune cell population
- $C(t)$, circulating lymphocyte population
- $M(t)$, chemotherapy drug concentration

The system of differential equations describing the growth, death, and interactions of these populations with a chemotherapy treatment is given by

$$\frac{dT}{dt} = aT(1 - bT) - c_1NT - K_TMT, \tag{1}$$

$$\frac{dN}{dt} = \alpha_1 - fN + g\frac{T}{h+T}N - pNT - K_NMN, \tag{2}$$

$$\frac{dC}{dt} = \alpha_2 - \beta C - K_CMC, \tag{3}$$

$$\frac{dM}{dt} = -\gamma M + V_M(t). \tag{4}$$

These equations have the general initial conditions $T(0) = T_0$, $N(0) = N_0$, $C(0) = C_0$, and $M(0) = M_0$, where each initial value is positive.

In Eq. (1), the tumor cell population is assumed to grow logistically, as justified in [16,17,15,18], while tumor cells are killed by the effector cells through a mass-action dynamic. In Eq. (2), the effector cells have a constant source rate α_1, while death is proportional to the population of effector cells through the term $-fN$. Effector cells are also recruited by tumor cells through a Michaelis–Menten term, $g\frac{T}{h+T}$, which serves to provide a saturation effect. Additionally, effector cells are inactivated through contact with tumor cells according to a mass-action dynamic. The circulating lymphocytes of Eq. (3) have a constant source rate α_2 and a proportional death term $-\beta C$. The chemotherapy concentration in Eq. (4) has an outside source term, $V_M(t)$, that represents treatment, and decays out of the system proportionally to the concentration through the term $-\gamma M$. In Eqs. (1)–(3), chemotherapy affects all three cell populations through a mass-action dynamic of the form K_JJ, $J = T, N, C$, with the differential effect of the medication on each cell type achieved through different values of the K_J parameters.

In Sections 4.1, 5.2 and 6 we present numerical experiments to explore certain dynamics of this model. For all the experiments presented, model parameters were set to the values given in Table 1. Most of the parameters used in these experiments were chosen to be within ranges that allowed for reasonable dynamics as well as convergence of the optimal control algorithm. Some of the parameters were taken from the literature, and these are noted in the table. At this stage, however, we accept that most parameter choices are not directly linked to experimental data since the focus of this paper is on the mathematical exploration of the development and comparison of the quadratic and linear optimal control problems. However, future work is planned to focus on connecting this model and the optimal control question more strongly to experimental data.

3. Dynamics

In order to understand the dynamics of the system (1)–(4), we identify the fixed points and determine their stability characteristics.

If $V_M(t)$ is a constant with value $V_M(t) = V_M$, then Eq. (4) implies $M = \frac{V_M}{\gamma}$. By substituting this result into Eq. (3), we have $C = \frac{\alpha_2\gamma}{\gamma\beta + K_CV_M}$. Also, Eq. (1) factors as $T[a(1 - bT) - c_1N - K_T M] = 0$. Therefore, at $T = 0$ there is an equilibrium point. If we substitute this value into Eq. (2), we get $N = \frac{\alpha_1\gamma}{\gamma f + K_NV_M}$.

Table 1
Estimated parameter values

Parameter	Units	Description	Estimated value	Source
a	day^{-1}	Tumor growth rate	4.31×10^{-3}	Estimated
b	cells^{-1}	1/b is tumor carrying capacity	1.02×10^{-14}	Estimated
c_1	$\text{cell}^{-1}\,\text{day}^{-1}$	Fractional tumor cell kill by effector cells	3.41×10^{-10}	Estimated
f	day^{-1}	Death rate of effector cells	4.12×10^{-2}	[45]
g	day^{-1}	Maximum effector cell recruitment rate by tumor cells	1.5×10^{-2}	[45,21]
h	cell^2	Steepness coefficient of the effector cell recruitment curve	2.02×10^{1}	Estimated
K_C, K_N	day^{-1}	Fractional effector cell and circulating lymphocyte kill by chemotherapy	6.00×10^{-1}	[59]
K_T	day^{-1}	Fractional tumor cell kill by chemotherapy	8.00×10^{-1}	[59]
p	$\text{cell}^{-1}\,\text{day}^{-1}$	Effector cell inactivation rate by tumor cells	2.0×10^{-11}	Estimated
α_1	$\text{cells}\,\text{day}^{-1}$	Constant source of effector cells	1.20×10^{4}	[45]
α_2	$\text{cells}\,\text{day}^{-1}$	Constant source of circulating lymphocytes	7.50×10^{8}	Estimated
β	day^{-1}	Death rate of circulating lymphocytes	1.20×10^{-2}	[1,36]
γ	day^{-1}	Rate of chemotherapy drug decay	9.00×10^{-1}	[6]

To analyze the stability of the $T = 0$ equilibrium, we take the Jacobian matrix of our system (1)–(4).

$$\begin{bmatrix} -2abT + a - c_1 N - K_T M & -c_1 T & 0 & -K_T T \\ -pN + gN\left(\frac{h}{(h+T)^2}\right) & -f - pT - K_N M + g\frac{T}{h+T} & 0 & -K_N N \\ 0 & 0 & -\beta - K_C M & -K_C C \\ 0 & 0 & 0 & -\gamma \end{bmatrix}.$$

The Jacobian evaluated at the equilibrium points $M = \frac{V_M}{\gamma}$, $C = \frac{\alpha_2 \gamma}{\gamma\beta + K_C V_M}$, and $N = \frac{\alpha_1 \gamma}{\gamma f + K_N V_M}$, gives

$$\begin{bmatrix} a - c_1 N - K_T M & 0 & 0 & 0 \\ -pN & -f - K_N M & 0 & -K_N N \\ 0 & 0 & -\beta - K_C M & -K_C C \\ 0 & 0 & 0 & -\gamma \end{bmatrix}.$$

Note that this matrix is block upper triangular. Furthermore, both the upper left 2×2 matrix and the lower right 2×2 matrix are themselves triangular, so the eigenvalues are

$$e_1 = a - c_1 N - K_T M = a - \frac{c_1 \alpha_1 \gamma}{\gamma f + K_N V_M} - \frac{K_T V_M}{\gamma},$$

$$e_2 = -f - K_N M = -f - \frac{K_N V_M}{\gamma},$$

$$e_3 = -\beta - K_C M = -\beta - \frac{K_C V_M}{\gamma},$$

$$e_4 = -\gamma.$$

With positive parameters, e_2, e_3, e_4 are all negative. Thus, the $T = 0$ equilibrium point is locally asymptotically stable whenever

$$a - \frac{c_1\alpha_1\gamma}{\gamma f + K_N V_M} - \frac{K_T V_M}{\gamma} < 0. \tag{5}$$

When $V_M = 0$ (no treatment), we find $T = 0$, $N = \frac{\alpha_1}{f}$, $C = \frac{\alpha_2}{\beta}$, and $M = 0$. Note that this point, with the given parameters, does not satisfy (5). However, when $V_M = 1$, then $M = 1/\gamma$, and the new fixed point $(T = 0, N = \frac{\alpha_1}{f+K_N/\gamma}, C = \frac{\alpha_2}{\beta+K_C/\gamma}, M = 1/\gamma)$ is stable. This reasonably implies that if the medicine is turned on the entire time, then the zero tumor equilibrium is stable.

Solving for the other zeros when $V_M = 0$ (no medicine) in Eq. (1) we obtain the following: $a(1 - bT)\left(f - \frac{gT}{h+T} + pT\right) - \alpha_1 c_1 = 0$, $N = \frac{\alpha_1}{\left(f - \frac{gT}{h+T} + pT\right)}$, $C = \frac{\alpha_2}{\beta}$, and M = 0.

The above equation for T reduces to a cubic,

$$a(1 - bT)((f + pT)(h + T) - gT) - c_1\alpha_1(h + T) = 0.$$

These equilibrium points and their stabilities were found numerically. Using Maple [51] to solve for T, we found, using the parameters of Table 1, that only one of the three roots to the cubic was physically meaningful; the other two roots implied a negative tumor size. The biologically meaningful equilibrium point was then analyzed using XPP [24], software for analysis of dynamical systems. XPP uses a generalized Newton method solver to find the fixed points of the system.

Using the parameter set given in Table 1, the values of the state variables at the fixed point were found to be $T = 9.8039 \times 10^{13}$, $N = 6.1199$, $C = 6.25 \times 10^{10}$ and $M = 0$. This fixed point has four real, negative eigenvalues which are $e_1 = -0.004324$, $e_2 = -1960.809617$, $e_3 = -0.012000$, and $e_4 = -0.900000$. Therefore, the system has a stable large tumor equilibrium and all orbits sufficiently close to this equilibrium point will tend to this large tumor fixed point.

In other words, through this result and the observations from simulations, we know that any tumor of size $T > 0$ will grow to this maximal tumor size. At this point, the tumor is so large, that it has reached the carrying capacity, and it cannot grow any further. If the tumor is not reduced, then the effector–immune cell population cannot sustain itself. In Eq. (2), we would have that the derivative becomes negative. Since this population N represents the immune system, then biologically this means that the immune system begins to fail.

We note that in the case of a non-zero tumor population with $V_M = 1$, the analysis yields equilibrium points only at negative cell populations. That is, there are no biologically meaningful T values for $V_M = 1$, so we do not pursue this case further.

4. Quadratic control

Given the model described in Section 2, we use the control V_M to decrease the tumor burden while minimizing total drug administered. We consider two different ways of quantifying this goal: a quadratic control and a linear control. In this section, we first analyze the theoretically more tractable quadratic control in order to present a clear picture of the process.

We minimize the objective functional,

$$J(V_M) = \int_0^{t_f} \left(T(t) + \frac{\epsilon}{2} V_M^2(t) \right) \mathrm{d}t.$$

subject to (1)–(4). First we, prove that there exists an optimal control that minimizes the objective functional. We use the fact that the supersolutions $\bar{T}, \bar{N}, \bar{C}, \bar{M}$ of

$$\begin{aligned} \frac{\mathrm{d}\bar{T}}{\mathrm{d}t} &= a\bar{T}, \quad \frac{\mathrm{d}\bar{N}}{\mathrm{d}t} = \alpha_1 + g\bar{N}, \\ \frac{\mathrm{d}\bar{C}}{\mathrm{d}t} &= \alpha_2, \quad \frac{\mathrm{d}\bar{M}}{\mathrm{d}t} = 1, \end{aligned} \tag{6}$$

are bounded on a finite time interval. Since the subsolutions are zero, then we can use a comparison result to obtain that our original system is bounded.

Since we have a bounded system, our next task is to establish the existence of the optimal control using a result from Fleming and Rishel [29, Corollary 4.1, p. 68].

Theorem 4.1 (Existence of a Quadratic Optimal Control). *Given the objective functional,* $J(V_M) = \int_0^{t_f} (T(t) + \frac{\epsilon}{2} V_M^2(t))\mathrm{d}t$, *where* $U = \{ V_M(t)$ *piecewise continuous* $|0 \leqslant V_M(t) \leqslant 1 \ \forall t \in [0, t_f] \}$ *subject to system (1)–(4) with* $T(0) = T_0$, $N(0) = N_0$, $C(0) = C_0$, $M(0) = M_0$ *then there exists an optimal control* V_M^* *such that* $\min_{V_M(t)\in[0,1]} J(V_M) = J(V_M^*)$ *if the following conditions are met*:

1. *The class of all initial conditions with a control* $V_M(t)$ *in the admissible control set along with each state equation being satisfied is not empty.*
2. *The admissible control set* U *is closed and convex.*
3. *Each right hand side of the state system is continuous, is bounded above by a sum of the bounded control and the state, and can be written as a linear function of* V_M *with coefficients depending on time and the state.*
4. *The integrand of* $J(V_M)$ *is convex on* U *and is bounded below by* $-c_2 + c_1 V_M^2$ *with* $c_1 > 0$.

Proof. By Fleming and Rishel [29], once we have proved conditions 1 through 4 above, we have existence.

Since the system (1)–(4) has bounded coefficients and the solutions are bounded on the finite time interval, we can use a result from Lukes [50], Theorem 9.2.1, page 182, to obtain the existence of the solution of the system (1)–(4). Secondly we note that U is closed and convex by definition. For the third condition, the right hand side of system (1)–(4) must be continuous. We see that only the right hand side of $\frac{\mathrm{d}N}{\mathrm{d}t}$ has a chance of being discontinuous. Since both h and T are positive this eliminates the possibility of $g\frac{T}{h+T}N$ being undefined. Therefore the entire system is continuous.

We let $\vec{\alpha}(t, \vec{X})$ be the right hand side of system (1)–(4) without $V_M(t)$ and let

$$\vec{f}(t, \vec{X}, V_M) = \vec{\alpha}(t, \vec{X}) + \begin{pmatrix} 0 \\ 0 \\ 0 \\ V_M \end{pmatrix}, \quad \text{with } \vec{X} = \begin{pmatrix} T \\ N \\ C \\ M \end{pmatrix}.$$

Using the boundedness of the solutions we see that

$$\left|\vec{f}(t,\vec{X},V_M)\right| \leqslant \left|\begin{pmatrix} a & 0 & 0 & 0 \\ 0 & g & 0 & 0 \\ 0 & 0 & 0 & 0 \\ 0 & 0 & 0 & 0 \end{pmatrix}\begin{pmatrix} T \\ N \\ C \\ M \end{pmatrix}\right| + \left|\begin{pmatrix} 0 \\ \alpha_1 \\ \alpha_2 \\ V_M \end{pmatrix}\right| \leqslant C_1\left(\left|\vec{X}\right| + |V_M|\right),$$

where C_1 depends on the coefficients of the system.

For the fourth condition we need to show

$$J(t,T,(1-p)u+pv) \leqslant (1-p)J(t,T,u) + pJ(t,T,v).$$

We analyze the difference of $J(t,T,(1-p)u+pv)$ and $(1-p)J(t,T,u)+pJ(t,T,v)$ to see that

$$\begin{aligned} &J(t,T,(1-p)u+pv) - [(1-p)J(t,T,u)+pJ(t,T,v)] \\ &\quad = T(t) + \frac{\epsilon}{2}\left(u^2 - 2pu^2 + p^2u^2 + p^2v^2 - 2p^2uv + 2pvu\right) - \left(T(t) + \frac{\epsilon}{2}u^2 - \frac{\epsilon}{2}u^2p + \frac{\epsilon}{2}pv^2\right) \\ &\quad = \frac{\epsilon}{2}(p^2-p)(u-v)^2. \end{aligned}$$

Since, $p \in (0,1)$ implies $(p^2-p) < 0$ and $(u-v)^2 > 0$, the expression $\frac{\epsilon}{2}(p^2-p)(u-v)^2$ is negative. This implies that $J(t,T,(1-p)u+pv) \leqslant (1-p)\ J(t,T,u) + pJ(t,T,v)$.

Lastly

$$T(t) + \frac{\epsilon}{2}V_M^2(t) \geqslant \frac{\epsilon}{2}V_M^2(t) \geqslant -c + \frac{\epsilon}{2}V_M^2(t)$$

which gives $-c + \frac{\epsilon}{2}V_M^2(t)$ as the lower bound. □

With the existence of the quadratic optimal control established, we now characterize the optimal control using the Pontryagin's Maximum Principle [60]. In the next theorem, we use $\frac{d\lambda_i}{dt} = \dot{\lambda}_i(t)$.

Theorem 4.2 (Characterization of the Optimal Control). *Given an optimal control V_M^* and solutions to the corresponding state system that minimize the functional $J(V_M) = \int_0^{t_f}(T(t) + \frac{\epsilon}{2}V_M^2(t))dt$, there exist adjoint variables λ_i for $i = 1,2,3,4$ satisfying*:

$$\begin{aligned} \dot{\lambda}_1 &= \lambda_1[2abT + c_1N + K_TM - a] + \lambda_2\left[pN - g\frac{h}{(h+T)^2}N\right] - 1, \\ \dot{\lambda}_2 &= \lambda_1c_1T + \lambda_2\left[f - g\frac{T}{h+T} + pT + K_NM\right], \\ \dot{\lambda}_3 &= \lambda_3[\beta + K_CM], \\ \dot{\lambda}_4 &= \lambda_1K_TT + \lambda_2K_NN + \lambda_3K_CC + \lambda_4\gamma, \end{aligned} \tag{7}$$

where $\lambda_i(t_f) = 0$ for $i = 1,2,3,4$. Moreover, $V_M^*(t)$ can be represented by

$$V_M^*(t) = \min\left(1, \left(-\frac{\lambda_4}{\epsilon}\right)^+\right),$$

where the notation is

$$r^+ = \begin{cases} r & \text{if } r \geqslant 0 \\ 0 & \text{if } r < 0. \end{cases}$$

Proof. For this functional, the Hamiltonian is given by

$$H = T + \frac{1}{2}\epsilon V_M^2 + \lambda_1[aT(1-bT) - c_1NT - K_TMT] + \lambda_2\left[\alpha_1 - fN + g\frac{T}{h+T}N - pNT - K_NMN\right] + \lambda_3[\alpha_2 - \beta C - K_CMC] + \lambda_4[-\gamma M + V_M]. \tag{8}$$

Since the control is bounded, we form the Lagrangian as follows:

$$\mathscr{L} = H + W_1(t)V_M(t) - W_2(t)(1 - V_M(t)).$$

Here H is the Hamiltonian as defined in (8) and $W_i(t) \geqslant 0$ are penalty multipliers such that $W_1(t)V_M(t) = 0$ and $W_2(t)(1 - V_M(t)) = 0$ at the optimal V_M^*.

To characterize V_M^*, we analyze the necessary optimality condition $\frac{\partial \mathscr{L}}{\partial V_M} = 0$. Here, $\frac{\partial \mathscr{L}}{\partial V_M} = \frac{\partial H}{\partial V_M} - W_1 + W_2 = 0$ or $\epsilon V_M + \lambda_4 - W_1 + W_2 = 0$.

Using standard optimality arguments, we characterize the optimal control for $V_M(t)$ as

$$V_M^*(t) = \min\left(1, \left(\frac{-\lambda_4}{\epsilon}\right)^+\right).$$

We also note that the second derivative of the Lagrangian with respect to V_M is positive, so a minimum occurs at V_M^*. □

4.1. Numerical simulations for quadratic control

The numerical solution of the quadratic control problem was achieved through two separate approaches. In the first, we implemented a two-point boundary value problem solver that we wrote in Matlab [53]. In the second, we used Miser3 [38], a commercial software package that interfaces with Matlab for solving optimal control problems. We chose to test our quadratic control problem using Miser3 in anticipation of the upcoming need for more sophisticated numerics to handle the linear control case. Both the Matlab code we wrote and Miser3 produced identical results. The parameter values used are given in Table 1.

In this numerical experiment, the system dynamics were run for 365 days. Fig. 1 pictures the cell population and medicine concentration levels for the first 100 days, since trends for the remaining days continue in the same way. In this case, the solution to the optimal control problem dictates that the medicine level, which is normalized to be between zero and one, should be initially high for a short period of time, after which it falls rapidly. The two immune cell populations continually increase over time, while the tumor cell population is quickly driven to a much lower level and is forced to remain there for the duration of the run. Although the end-time tumor population is far below that which would be considered clinically detectable in most cases, on the order of

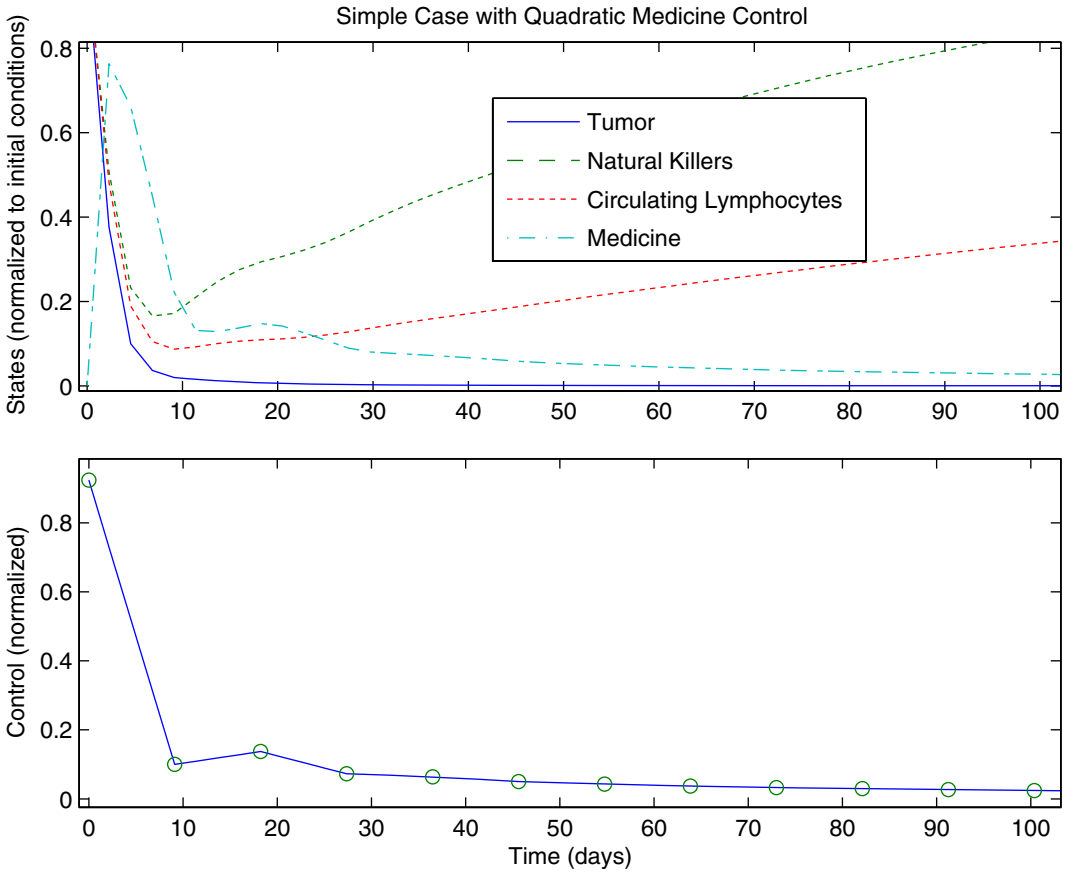

Fig. 1. Quadratic control situation. This is a 100 day view of optimal chemotherapy treatment for 365 days. One can see that the largest dose of (normalized) chemotherapy is administered at the beginning of the time period, and then is lowered to a small but non-zero and very slowly decreasing level for the remainder of the treatment period. The tumor is driven to near-zero, while the populations of immune cells are rising. Initial tumor size is 1×10^7 cells. Initial natural killer cell level is 3×10^5 and initial circulating lymphocyte level is 6.25×10^{10}.

8×10^2 cells, the cell population is still non-zero. As was seen from the analysis in Section 3, the zero-tumor fixed point of the system in not stable in this case. Once the low-dose of medicine is shut off, the tumor population is expected to re-grow, eventually. Clinically, this might be interpreted to mean that in this case, with this particular control, a patient would be required to take regular low-dose medication for the remainder of his or her life. We note that the control found by Miser3 matches the characterization given in Theorem 4.2.

5. Linear control

For the same model (1)–(4), we now minimize an objective functional that is linear in the control,

$$J_1(V_M) = \int_0^{t_f} (T(t) + \epsilon V_M(t))\mathrm{d}t. \tag{9}$$

This objective functional depicts the situation of minimizing the tumor cells and the total amount of drug given for a time interval $[0, t_f]$.

5.1. Characterization of control

The existence of a linear control can be shown by techniques similar to those presented in Section 4.1. Assuming the existence of such a control, we develop the characterization. The added benefit given by the following analysis is a new graphical display of the regions on which the singular arc is optimal. See Fig. 2.

Theorem 5.1 (Characterization of the Optimal Control). *Given an optimal control* $V_M^*(t)$, *and solutions to the state equations that minimize the functional* $J_1(V_M) = \int_0^{t_f} (T(t) + \epsilon V_M(t))\mathrm{d}t$, *there*

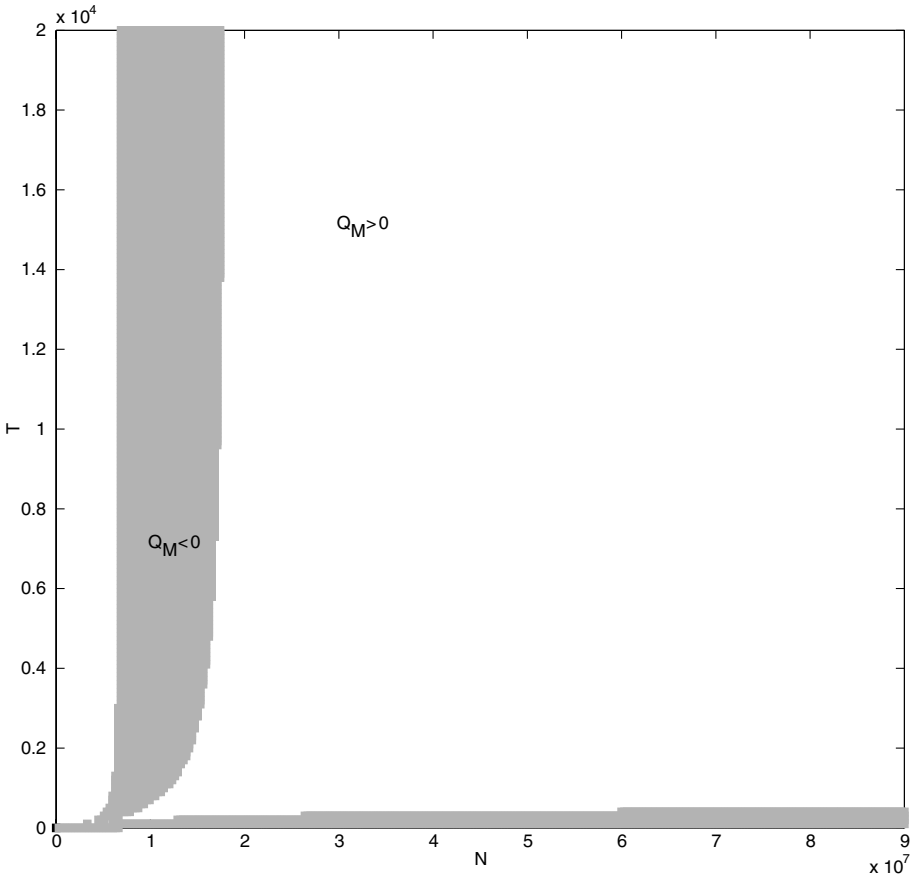

Fig. 2. Plot of $Q(T, N)$. Here, Q is denoted by Q_M in the graphic. Q is negative in the shaded region. This says that the singular control is minimizing in the unshaded regions.

exist adjoint variables satisfying the adjoint Eq. (7) with $\lambda_i(t_f) = 0$ *for* $i = 1, 2, 3, 4$. *Further, the optimal control is characterized by*

$$V_M = \begin{cases} 0 & \text{if } \epsilon + \lambda_4 > 0 \\ 1 & \text{if } \epsilon + \lambda_4 < 0 \\ -\frac{P(T,N,M)}{Q(T,N)} & \text{if } \epsilon + \lambda_4 = 0 \end{cases}$$

where

$$\begin{aligned} Q(T,N) &= K_T^2 T - \lambda_1 (K_T^2 abT^2 + c_1 K_N^2 NT) \\ &\quad + \lambda_2 \left(\alpha_1 K_N^2 - K_T^2 NT \left(p - \frac{gh}{(h+T)^2} + \frac{2ghT}{(h+T)^3} \right) \right) \quad \text{and} \\ P(T,N,M) &= \left[\lambda_1 \frac{\partial \mu_1}{\partial T} + \lambda_2 \frac{\partial \mu_2}{\partial T} + (K_T - K_N) c_1 N - K_T (a - K_T M) \right] \dot{T} \\ &\quad + \left[\lambda_1 \frac{\partial \mu_1}{\partial N} + \lambda_2 \frac{\partial \mu_2}{\partial N} + c_1 (K_T - K_N) T \right] \dot{N} \\ &\quad + \mu_1 \dot{\lambda_1} + \mu_2 \dot{\lambda_2} - \gamma QM. \end{aligned}$$

Proof. In this case, the Hamiltonian of the system is given by

$$\begin{aligned} H &= T + \epsilon V_M + \lambda_1 [aT(1 - bT) - c_1 NT - K_T MT] + \lambda_2 \left[\alpha_1 - fN + g \frac{T^\eta}{h + T^\eta} N - pNT - K_N MN \right] \\ &\quad + \lambda_3 [\alpha_2 - \beta C - K_C MC] + \lambda_4 [-\gamma M + V_M]. \end{aligned}$$

The switching function in this case is $\phi = \frac{\partial H}{\partial V_M} = \epsilon + \lambda_4$. Since there is no explicit dependence on V_M in the switching function, the possibility of singular arcs arises.

The optimal control is given by

$$V_M = \begin{cases} 0 & \text{if } \epsilon + \lambda_4 > 0 \\ 1 & \text{if } \epsilon + \lambda_4 < 0 \\ \text{Singular} & \text{if } \epsilon + \lambda_4 = 0. \end{cases}$$

In the regions where the switching function is not zero, we have bang–bang control. In order to address the issue of singular arcs, we suppose the switching function is zero on an interval (t_1, t_2). This implies that all the derivatives of λ_4 must vanish in that interval. We can use this fact to determine the optimal control in such regions.

For the explanation to follow, we recall that $\dot{\lambda_3} = \lambda_3[\beta + K_C M]$. Since $M(t) \geqslant$ and $\lambda_3(t_f) = 0$, we can conclude that $\lambda_3(t) = 0$ on the entire time interval. Setting the first three time derivatives of the switching function to zero, and using $\lambda_3 \equiv 0$, we obtain

$$\begin{aligned} \dot{\phi} &= 0 = \lambda_1 K_T T + \lambda_2 K_N N - \gamma \epsilon, \\ \ddot{\phi} &= 0 = \lambda_1 (K_T abT^2 + c_1 K_N NT) + \lambda_2 \left(\alpha_1 K_N - \frac{K_T ghTN}{(h+T)^2} + K_T pNT \right) - K_T T \quad \text{and} \\ \dddot{\phi} &= 0 = \lambda_1 \mu_1 + \lambda_2 \mu_2 - (K_T T(a - c_1 N - K_T M) + c_1 K_N NT), \end{aligned}$$

where

$$\mu_1(T,N,M) = T^2[K_T ab(a - K_T M) + c_1(p - ab)(K_T - K_N)N] + c_1 K_N T(2\alpha_1 - fN - K_N MN) - \frac{c_1 K_T ghT^2 N}{(h+T)^2} + \frac{c_1 g K_N N T^2}{h+T} \quad \text{and}$$

$$\mu_2(T,N,M) = -\frac{\alpha_1 K_N gT}{(h+T)} - \frac{ghT}{(h+T)^2}(K_T abTN + c_1 K_N N^2 + K_T \alpha_1) - \frac{ghK_T N}{(h+T)^3}(h-T)(aT(1-bT) - c_1 NT - K_T MT) + c_1 pN^2 T(K_N - K_T) + \alpha_1 K_N f + \alpha_1 pT(K_N + K_T) + K_T pNT(a - K_T M) + \alpha_1 K_N^2 M.$$

From $\dot{\phi} = 0$ and $\ddot{\phi} = 0$, we can solve for λ_1 and λ_2 in terms of the state. We get

$$\lambda_1 = \frac{K_N K_T NT - \gamma\epsilon(\alpha_1 K_N - \frac{K_T ghTN}{(h+T)^2} + K_T pNT)}{(K_N K_T abT^2 N + c_1 K_N^2 N^2 T - K_T T(\alpha_1 K_N - \frac{K_T ghTN}{(h+T)^2} + K_T pNT))} \quad \text{and}$$

$$\lambda_2 = \frac{\gamma\epsilon(K_T abT^2 + c_1 K_N NT) - K_T^2 T^2}{(K_N K_T abT^2 N + c_1 K_N^2 N^2 T - K_T T(\alpha_1 K_N - \frac{K_T ghTN}{(h+T)^2} + K_T pNT))}.$$

Now we know all four adjoint variables in terms of the state in a singular region. To determine the control, we need to find the fourth derivative of the switching function.

We then get a linear equation in V_M whose coefficients are functions of T, N and M. We see that $\dddot{\phi} = 0 = Q(T,N)V_M + P(T,N,M)$ or $V_M = -\frac{P(T,N,M)}{Q(T,N)}$ where

$$Q(T,N) = K_T^2 T - \lambda_1(K_T^2 abT^2 + c_1 K_N^2 NT) + \lambda_2\left(\alpha_1 K_N^2 - K_T^2 NT\left(p - \frac{gh}{(h+T)^2} + \frac{2ghT}{(h+T)^3}\right)\right) \quad \text{and}$$

$$P(T,N,M) = \left[\lambda_1\frac{\partial\mu_1}{\partial T} + \lambda_2\frac{\partial\mu_2}{\partial T} + (K_T - K_N)c_1 N - K_T(a - K_T M)\right]\dot{T} + \left[\lambda_1\frac{\partial\mu_1}{\partial N} + \lambda_2\frac{\partial\mu_2}{\partial N} + c_1(K_T - K_N)T\right]\dot{N} + \mu_1\dot{\lambda_1} + \mu_2\dot{\lambda_2} - \gamma QM.$$

Here $\dot{T}$, $\dot{N}$, $\dot{\lambda_1}$ and $\dot{\lambda_2}$ are given by the relevant expressions for the time derivative in the state and adjoint equations and

$$\frac{\partial\mu_1}{\partial T} = 2T(K_T ab(a - K_T M) + c_1(p - ab)(K_T - K_N)N) + c_1 K_N(2\alpha_1 - fN - K_N MN) + c_1 g K_N NT\frac{(2h+T)}{(h+T)^2} - c_1 ghK_T NT\frac{(2h)}{(h+T)^3},$$

$$\frac{\partial\mu_1}{\partial N} = c_1(p - ab)(K_T - K_N)T^2 - c_1 K_N^2 MT - \frac{c_1 ghK_T T^2}{(h+T)^2} + \frac{c_1 g K_N T^2}{h+T},$$

$$\frac{\partial\mu_2}{\partial T} = -\frac{gh(\alpha_1 K_N + K_T abNT)}{(h+T)^2} + pc_1 N^2(K_N - K_T) + p\alpha_1(K_N + K_T)$$

$$- gh(\alpha_1 K_T + c_1 K_N N^2)\frac{(h-T)}{(h+T)^3} + pK_T N(a - K_T M)$$
$$- \frac{ghK_T N(a - abT - c_1 N - K_T M)(T - 4hT + h^2)}{(h+T)^4} \quad \text{and}$$

$$\frac{\partial \mu_2}{\partial N} = -gh\frac{T}{(h+T)^2}(K_T abT + 2c_1 K_N N) + 2c_1 pNT(K_N - K_T)$$
$$+ K_T pT(a - K_T M) - ghK_T\frac{T(h-T)}{(h+T)^3}(a(1-bT) - 2c_1 N - K_T M).$$

Since we know λ_1 and λ_2 in terms of the state variables T and N, we know Q purely in terms of T and N. For the singular control to be minimizing, the Generalized Legendre Clebsch condition needs to be satisfied, that is $Q(T,N)$ would have to be non-negative on this interval. The plot is shown in Fig. 2. Note that $Q(T,N)$ is only negative in a very specific region. In this region, we can guarantee that there are no singular minimizing arcs, so the control is bang–bang. In other regions, the potential for singular arcs has not been ruled out, but in fact arises in most practical situations, since most of the T–N plane meets the criterion $Q(T,N) \geqslant 0$. □

5.2. Numerical simulations for linear control

We used Miser3 to find numerically the optimal control minimizing the functional

$$J(V_M) = \int_0^{t_f}\left(\frac{T(t)}{T_0} + V_M(t)\right)\mathrm{d}t, \tag{10}$$

with the parameters as given in Table 1.

The initial tumor concentration has order of magnitude 7, while the control V_M has order of magnitude 0. Therefore, for numerical purposes, we have normalized the tumor population T by the initial condition T_0, so that the initial value of T is 1, and the quantity $T(t)/T_0$ is tracked. This allows us to display more clearly the dynamics of the system within one set of plots for each scenario.

Fig. 3 shows a run of Miser3 which gives a 365 day treatment, applying a short burst of chemotherapy in the beginning which allows the immune cell populations to recover after a few days, while driving the tumor to a low of about 1.4×10^4 cells around day 14, after which the tumor population begins to increase again. However, the rate of increase is so slow that it is nearly imperceptible, and certainly not visually apparent. By day 365, the tumor population is at 6.0×10^4 cells, which is still considered clinically undetectable in many cases. As in the case of the quadratic control, since the zero-tumor equilibrium is not stable for this parameter set, the clinical implication of this kind of treatment is that tumor size would be maintained at a very low level, perhaps over the longer term with intermittent and widely spaced reapplications of chemotherapy, without ever actually eliminating the tumor. The optimal control in this run appears to be bang–bang. The switching occurs when the costate λ_4 crosses the value $\epsilon_M = 1$ (that is $\lambda_4 + 1$ becomes positive) at 9.125 days.

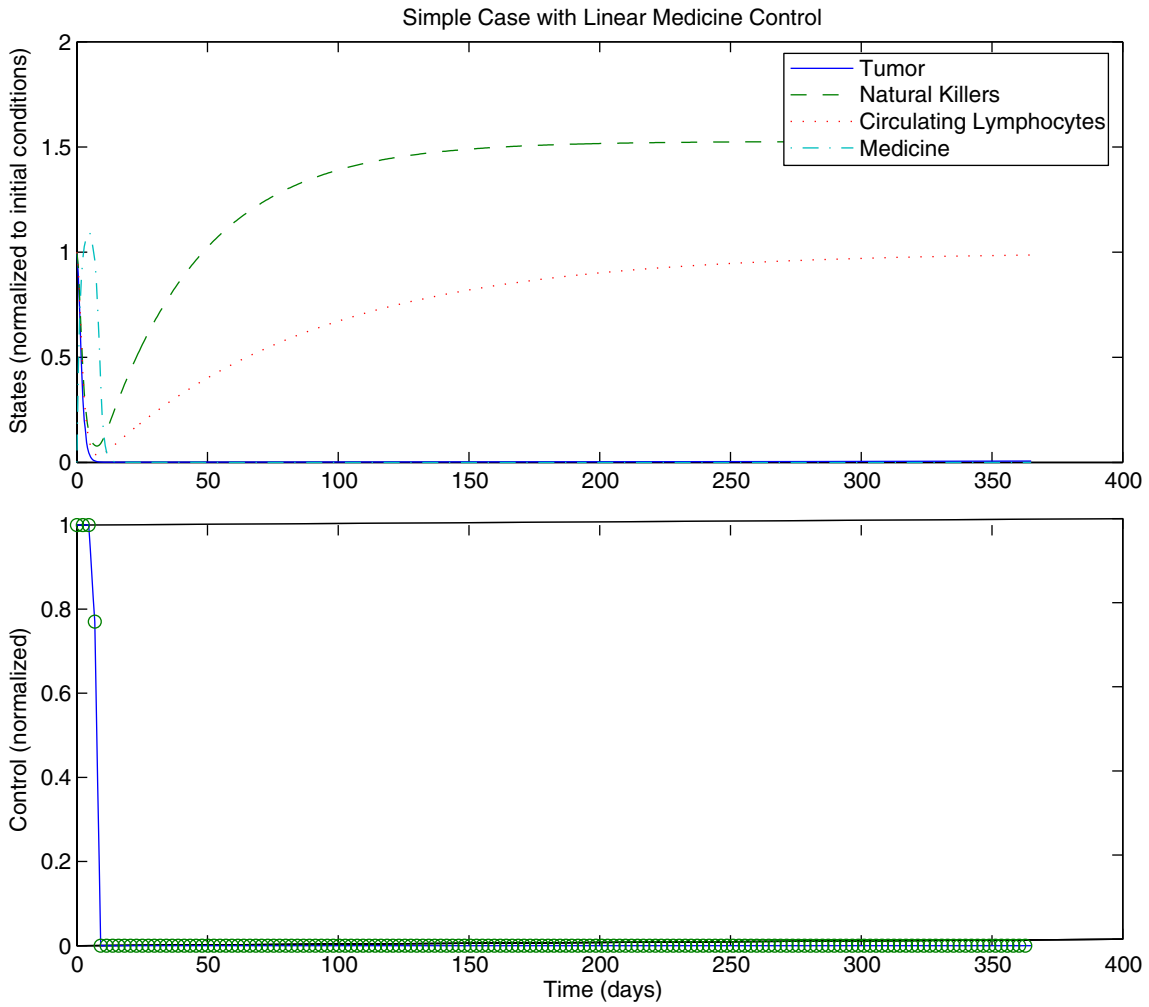

Fig. 3. These graphs represent the states and control for the linear case. There is an initial burst of chemotherapy at the start of the treatment period, after which the medicine is completely shut off and is never again turned on. The tumor is driven to a very low but non-zero level, while the immune cell populations increase over time. Initial tumor size is 1×10^7 cells. Initial natural killer cell level is 3×10^5 and initial circulating lymphocyte level is 6.25×10^{10}.

Note that in Fig. 3 there is a single point for which the medicine dose takes on a value other than zero or one. The presence of this single point does not necessarily indicate the existence of a true singular region, but is more likely to be a numerical artifact generate by the approach Miser3 uses to solve the problem.

We also see that because the medicine only remains in the patient's system for a few days, the immune system has a chance to recover. Both the circulating lymphocytes and natural killer cells return to normal levels after the chemotherapy is turned off. This strong immune system keeps the tumor regrowth rate low over the 365 day period.

The second Miser3 run had the same objective functional $J(V_M)$ as in Eq. (10). However, this time, the final time was allowed to be free, and an optimal final time was automatically found by

the software. The Miser3 software can search numerically for an optimal final time by transforming the problem into a canonical problem form, which in turn is addressed as a combined optimal parameter selection and optimal control problem. In particular, the unspecified terminal time problem is one in which the problem is defined over the interval $[t_0, t_f]$ and t_f is free to vary. In this case, Miser3 treats t_f as an unknown system parameter, maps the interval $[t_0, t_f]$ onto $[0, 1]$, and optimizes the transformed problem. Further details may be found in [38].

In Fig. 4, the time axis is normalized to 1. Miser3 chose the maximum allowable time (365 days) as configured before the run to be the optimal treatment length. Therefore, because Miser3 chose the same number of days as in the previous fixed-final-time run, we see the results are much the same. This is because the tumor in this case is reduced by the control, so then the average tumor size is lower if the run-time of the simulation is longer. Again, a short burst of chemotherapy in

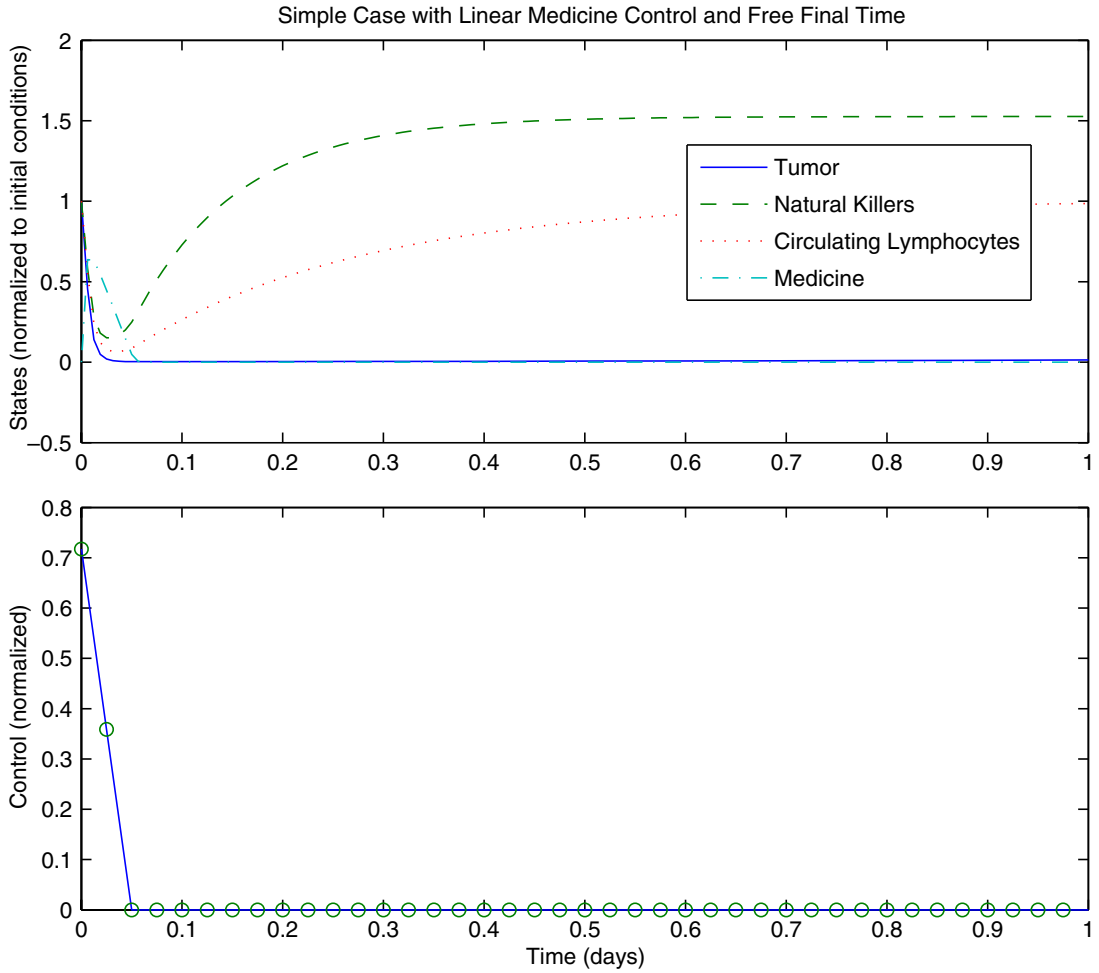

Fig. 4. Linear medicine control with free final time. Three hundred and sixty-five days was found to be the optimal time. A single initial dose of chemotherapy is sufficient to control the tumor. Initial tumor size is 1×10^7 cells. Initial NK cell level is 3×10^5 and initial circulating lymphocyte level is 6.25×10^{10}.

the very beginning was enough to control the tumor; and because the drug only lasts in the patient's system for a few days, the immune system has a chance to recover.

With this functional, V_M will always turn on for an interval at the very beginning of the run. This is reasonable, since we are minimizing the amount of drug $V_M(t)$ over the entire time interval. In other words, turning on the medicine at the beginning will reduce the tumor so that the average tumor size in our simulations over the entire period is small. It is possible that the lower effector–immune cell count resulting from the treatment allows the tumor to grow more quickly than it would have had we waited to give treatment. This is highly unlikely, however, because larger tumor sizes have been shown in our simulations to suppress effector–immune cell activity. This is a reasonable reflection of the biology, since it is known that one way in which tumors evade rejection by the immune system is to secrete immunosuppressive cytokines [37, p. 637] that in turn downregulate T-cell responses and cell-mediated immunity.

In our simulations, a singular control for V_M was not encountered. Referring to Fig. 2, we note that the parameters of the problem are such that the singular control remained in the region in which it was not optimal.

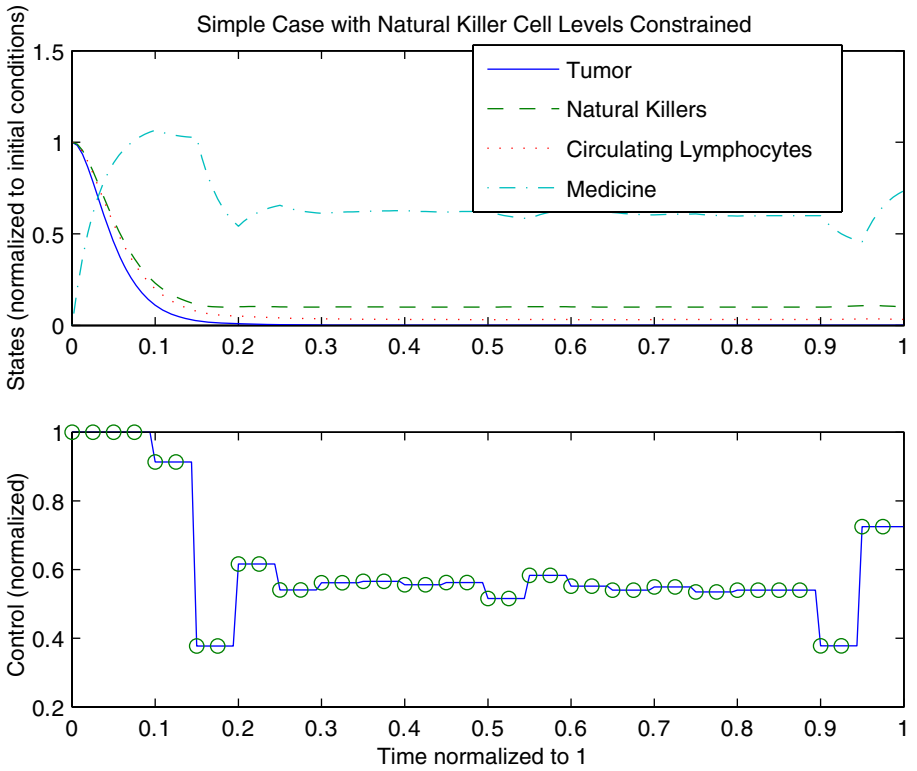

Fig. 5. In this run, the only value minimized was the tumor size. Additionally, the natural killer cells were required to be kept above 10% of their initial value and final time was not fixed. Miser chose 35.62 days to run this simulation. The medicine starts high and then lowers and adjusts to keep the natural killer cells at the appropriate level. Initial tumor size is 1×10^7cells. Initial natural killer cell level is 3×10^5 and initial circulating lymphocyte level is 6.25×10^{10}.

6. Optimal control with state constraint

In the following numerical experiment, rather than minimizing the tumor and the medicine, as in the linear and quadratic simulations, here the objective functional only includes the tumor,

$$J_2 = \int_0^{t_f} T \mathrm{d}t.$$

Therefore, in order to keep the virtual patient reasonably 'healthy', a state constraint was set in Miser3 so that the immune cell levels remained above 10% of their initial value. Additionally, the final time was free in this simulation, allowing Miser to choose the best final time, which in this case was 35.62 days. See Fig. 5.

The consequences of this functional change are two-fold. First, the medicine is never turned off. This is because there is no penalty in the objective functional for having the medicine on, as long as the natural killer cells are at an appropriate level. Second, there is a piecewise continuous optimal control function for the chemotherapy treatment. Here the minimizing control is singular, and the singular control is piecewise linear. Clinically, this type of treatment may be very difficult to administer. However, if it were possible to allow a patient to carry with them some sort of medicine pump, the implication with this state-constrained control problem is that it may be possible to eliminate the tumor within a much shorter period of time than in the cases presented previously.

7. Conclusion

For the two types of objective functionals analyzed, optimal controls were explicitly characterized. Treatments based on both functionals were successful in reducing the tumor to near zero. Numerical simulations agreed with the theoretical characterization of the optimal controls.

The quadratic and linear controls have similar behavior in the administration of the chemotherapy drug. They are both turned on at full power ($V_M = 1$) for a short period of time, then they are essentially turned off. In the linear control it is completely turned off. However in the quadratic case, the control quickly moves to a small value, then gradually decreases. Since the amount of drug being delivered to the patient is small, the quadratic control treatment is comparable to the linear bang–bang control case in that the tumor is reduced by the same magnitude over the same time frame. However, the quadratic control has the added benefit of keeping the tumor in check when it is small. When the tumor is small, the strongest treatment of the tumor is unnecessary. The quadratic control allows for a weaker treatment that minimizes the harmful side-effects while allowing the system to maintain a low tumor size.

Likewise, the state-constrained control situation in Fig. 5 generates a chemotherapy regimen that gives a full dose of treatment at the beginning. At later times, the drug is given at levels that decrease tumor while maintaining a minimum natural killer cell population. However, the control is segregated into multiple pieces that represent constant drug treatment on those intervals.

Overall, the model demonstrates that a burst of treatment at the beginning is the best way to fight the tumor. If enough medicine can be administered to kill the tumor quickly and push the

state variables toward the zero-tumor equilibrium, then the cancer can be controlled effectively. This coincides with previous work by Murray [55] in which he studied a cancer model with a normal cell population. He found that the optimal solution included a bolus application of the drug followed later by continuous infusion. In the quadratic and linear cases, we found essentially the same concepts. In the clinical setting, Gurney states that an injection is administered that is based on the body surface area. Gurney [34] states that a fixed dose can be given, yet the prescribed initial dose is inaccurate 40% of the time. Therefore, Gurney recommends employing a range of fixed doses that could be used as a starting dose and for alterations thereafter. In the state constrained case, the drug is given at the highest level, roughly constant in the middle portion of the treatment, and then increased to approximately 70% of the maximal level of treatment. Within our work, we have shown that this reduces the tumor burden to almost zero. But, we cannot say that the tumor is eradicated. Work by Kutznetsov and Knott [44] conclude this as well. Their experimental results confirm the clinical observations that inclusion of immune cells does not provide complete tumor elimination. Their suggestion is to introduce immune memory cells. In work under preparation, we are incorporating such an immune cell situation to determine whether we can move the system to a stable equilibrium with the use of chemotherapy and vaccination therapy.

The main contributions of this paper involve the use of two immune cell populations included in the dynamics to reduce the tumor burden, the qualitative results for quadratic and linear optimal control scenarios, and the graphical display of the representation of the a minimal singular arc. Since singular representations are difficult to determine, the ability to produce a representation for a highly coupled model and to depict the regions on which a singular control is optimal are significant. The numerical results give insight into the different chemotherapy situations that can occur with the addition of immune cell populations and state constraints. The biological aspect of giving maximal drug for the initial dose and then providing a continuous infusion of drug in the non-constrained cases means that the tumor burden is reduced drastically and the immune cells are suppressed for approximately the first 20 days. Subsequently the effector–immune cells and the circulating lymphocytes recover to approximately 80% and 40% of their original levels in the quadratic case. In the linear non-constrained case, the effector cells increase to 50% above their original level and the circulating lymphocytes return to their initial value. This may imply that the drug reduces the tumor burden and then the immune cells act as inhibitors to cancer regrowth [23]. In the constrained linear case, we see that the effector–immune cells and the circulating lymphocytes do not recover. Therefore, as described in the previous paragraph, the chemotherapy dosage is given for the entire period with fluctuating fixed amounts. In accordance with the literature, the immune cells are not able to keep the tumor in check and chemotherapy is needed to do so. In future work, investigations into more complex models will address the ability of combined immunotherapy and chemotherapy to control the tumor burden and hopefully to eradicate the cancer.

Acknowledgments

We thank the referees for the careful reading of this manuscript, the questions they posed and suggestions they offered. As a result, this paper is significantly improved.

Appendix

We state two theorems which arise in the discussion of the characterization of the quadratic and linear control scenarios, respectively. We also comment on the use of Miser3.

Theorem 9.1 (Pontryagin's Minimum Principle [60]). *For the control* $\vec{u} = (u_1, \ldots, u_m)'$ *belonging to the admissible control set* U *and related trajectory* $\vec{x} = (x_1, \ldots, x_n)'$ *that satisfies*

$$\dot{x}_i = g_i(\vec{x}, \vec{u}, t) \qquad \text{(state equations)},$$
$$x_i(a) = c_i \qquad \text{(initial conditions)}$$

but with free end conditions, to minimize the performance criterion

$$J = \psi(\vec{x}, t)|_a^b + \int_a^b f(\vec{x}, \vec{u}, t)\mathrm{d}t$$

it is necessary that a vector $\vec{\lambda} = \vec{\lambda}(t)$ *exist such that*

$$\dot{\lambda}_i = -\frac{\partial H}{\partial x_i} \qquad \text{(adjoint equations)},$$
$$\lambda_i(b) = \psi_{x_i}[\vec{x}(b), b] \qquad \text{(adjoint final conditions)},$$

where the Hamiltonian

$$H = f + \sum_{i=1}^{n} \lambda_i g_i$$

for all t, $a \leqslant t \leqslant b$, *and all* $\vec{v} \in U$, *satisfies*

$$H[\vec{\lambda}(t), \vec{x}(t), \vec{v}] \geqslant H[\vec{\lambda}(t), \vec{x}(t), \vec{u}(t)].$$

For the discussion of singular arcs, we used the following theorem.

Theorem 9.2 (Generalized Legendre Clebsch Conditions[43]). *Suppose the controls* u_i *for* $i = 1, 2, \ldots, n$ *are singular on an interval. Let* A *be the* $n \times n$ *matrix given by*

$$A_{ij} = (-1)^{q_j} \frac{\partial}{\partial u_i} \frac{\mathrm{d}^{q_i + q_j}}{\mathrm{d}t^{q_i + q_j}} \frac{\partial H}{\partial u_j},$$

where q_i *is the order of the singularity of the control* u_i. *Then* A *must be non-negative definite for the control to be minimizing. If there is only one control,* u_i, *that is singular, this reduces to*

$$(-1)^{q_i} \frac{\partial}{\partial u_i} \frac{\mathrm{d}^{2q_i}}{\mathrm{d}t^{2q_i}} \frac{\partial H}{\partial u_i} \geqslant 0.$$

For the numerical experiments for quadratic and linear controls, we developed our own Matlab [53] code and made comparisons with commercial code Miser3 [38]. Before choosing Miser3, we tested other software packages, including RIOTS [62] and DIRCOL [69], in order to compare the efficacy and usability of these commonly available packages. RIOTS, which runs with Matlab on a Windows platform only, was very parameter sensitive, and could not easily handle the state

constraint case. DIRCOL, which is Fortran based and can run on any platform with a Fortran compiler, can handle a wide variety of cases as well as state constraints, but the implementation of a linear control is very tricky. Miser3, which runs with Matlab under Windows or Linux, is able to handle quadratic and linear controls as well as state constraints, however the state-constrained case ran very slowly. We found that there is no perfect package, but we were satisfied with the results generated by Miser3.

References

[1] L. Bannock, Nutrition. Available from: <http://www.doctorbannock.com/nutrition.html>.
[2] N. Bellomo, A. Bellouquid, M. Delitala, Mathematical topics on the modelling of multicellular systems in competition between tumor and immune cells, Math. Mod. Meth. Appl. Sci. 14 (2004) 1683.
[3] N. Bellomo, L. Preziosi, Modelling and mathematical problems related to tumor evolution and its interaction with the immune system, Math. Comput. Model. 32 (2000) 413.
[4] J.N. Blattman, P.D. Greenberg, Cancer immunotherapy: a treatment for the masses, Science 305 (July) (2004) 200.
[5] Thalya Burden, Jon Ernstberger, K. Renee Fister, Optimal control applied to immunotherapy, Discrete Contin. Dyn. Syst. Ser. B 4 (1) (2004).
[6] P. Calabresi, P.S. Schein (Eds.), Medical Oncology: Basic Principles and Clinical Management of Cancer, second ed., McGraw-Hill, New York, 1993.
[7] R.Y. Chandawarkar, D.P. Guyton, Oncologic mathematics – evolution of a new specialty, Arch Surg. 137 (2002) 1428.
[8] K.A. Chester, A. Mayer, J. Bhatia, L. Robson, D.I.R. Spencer, S.P. Cooke, A.A. Flynn, S.K. Sharma, G. Boxer, R.B. Pedley, R.H.J. Begent, Recombinant anti-carcinoembryonic antigen antibodies for targeting cancer, Cancer Chemother. Pharmacol. 46 (2000) S8.
[9] Andrew J. Coldman, J.M. Murray, Optimal control for a stochastic model of cancer chemotherapy, Math. Biosci. 168 (2) (2000) 187.
[10] J. Couzin, Select T cells, given space, shrink tumors, Science 297 (September) (2002) 1973.
[11] S.B. Cui, Analysis of a mathematical model for the growth of tumors under the action of external inhibitors, J. Math. Biol. 44 (2002) 395.
[12] A. Dalgleish, The relevance of non-linear mathematics (chaos theory) to the treatment of cancer, the role of the immune response and the potential for vaccines, QJM 92 (1999) 347.
[13] E. De Angelis, P.E. Jabin, Qualitative analysis of a mean field model of tumor–immune system competition, Math. Mod. Meth. Appl. Sci. 13 (2003) 187.
[14] E. De Angelis, L. Mesin, Modelling of the immune response: conceptual frameworks and applications, Math. Mod. Meth. Appl. Sci. 11 (2001) 1609.
[15] L.G. de Pillis, W. Gu, A.E. Radunskaya, Mixed immunotherapy and chemotherapy of tumors: modeling, applications and biological interpretations, J. Theor. Biol. 238 (4) (2006) 841.
[16] L.G. de Pillis, A.E. Radunskaya, A mathematical tumor model with immune resistance and drug therapy: an optimal control approach, J. Theor. Med. 3 (2001) 79.
[17] L.G. de Pillis, A.E. Radunskaya, The dynamics of an optimally controlled tumor model: a case study, Math. Comput. Model. 37 (11) (2003) 1221.
[18] L.G. de Pillis, A.E. Radunskaya, C.L. Wiseman, A validated mathematical model of cell-mediated immune response to tumor growth, Cancer Res. 61 (17) (2005) 7950.
[19] M. Delitala, Critical analysis and perspectives on kinetic (cellular) theory of immune competition, Math. Comput. Model. 35 (2002) 63.
[20] L. Derbel, Analysis of a new model for tumor–immune system competition including long time scale effects, Math. Mod. Meth. Appl. Sci. 14 (2004) 1657.
[21] A. Diefenbach, E.R. Jensen, A.M. Jamieson, D. Raulet, Rae1 and H60 ligands of the NKG2D receptor stimulate tumor immunity, Nature 413 (September) (2001) 165.

[22] J. Donnelly, Cancer vaccine targets leukemia, Nat. Med. 9 (11) (2003) 1354.
[23] A. d'Onofrio, A general framework for modeling tumor-immune system competition and immunotherapy: mathematical analysis and biomedical references, Physica D 208 (2005) 220.
[24] Bard Ermentrout, Simulating, Analyzing, and Animating Dynamical Systems: A Guide to XPPAUT for Researchers and Students, SIAM, 2002.
[25] S.C. Ferreira, M.L. Martins, M.J. Vilela, Reaction-diffusion model for the growth of avascular tumor, Phys. Rev. E 65 (2002).
[26] K.R. Fister, J. Donnelly, Immunotherapy: an optimal control theory approach, Math. Biosci. Eng. 2 (3) (2005) 499.
[27] K. Renee Fister, John Carl Panetta, Optimal control applied to cell-cycle-specific cancer chemotherapy, SIAM J. Appl. Math. 60 (3) (2000) 1059.
[28] K. Renee Fister, John Carl Panetta, Optimal control applied to competing chemotherapeutic cell-kill strategies, SIAM J. Appl. Math. 63 (6) (2003) 1954.
[29] Wendell H. Fleming, Raymond W. Rishel, Deterministic and Stochastic Optimal Control, Springer-Verlag, 1975.
[30] S.W. Friedrich, S.C. Lin, B.R. Stoll, L.T. Baxter, L.L. Munn, R.K. Jain, Antibody-directed effector cell therapy of tumors: analysis and optimization using a physiologically based pharmacokinetic model, Neoplasia 4 (2002) 449.
[31] P. Garcia-Penarrubia, N. Lorenzo, J. Galvez, A. Campos, X. Ferez, G. Rubio, Study of the physical meaning of the binding parameters involved in effector-target conjugation using monoclonal antibodies against adhesion molecules and cholera toxin, Cell Immunol. 215 (2002) 141.
[32] R.A. Gatenby, E.T. Gawlinski, The glycolytic phenotype in carcinogenesis and tumor invasion: insights through mathematical models, Cancer Res. 63 (2003) 3847.
[33] R.A. Gatenby, P.K. Maini, Modelling a new angle on understanding cancer, Nature 410 (December) (2002) 462.
[34] H. Gurney, How to calculate the dose of chemotherapy, Brit. J. Cancer 86 (2002) 1297.
[35] K. Hardy, J. Stark, Mathematical models of the balance between apoptosis and proliferation, Apoptosis 7 (2002) 373.
[36] B. Hauser, Blood tests. Technical report, International Waldenstrom's Macroglobulinemia Foundation. Available from: <http://www.iwmf.com/Blood_Tests.pdf>, January 2001 (accessed May 2005).
[37] C.A. Janeway, P. Travers, M. Walport, M.J. Shlomchik, Immunobiology: The Immune System in Health and Disease, sixth ed., Garland Science Publishing, 2005.
[38] L.S. Jennings, M.E. Fisher, K.L. Teo, and C.J. Goh, MISER3 Optimal Control Software: Theory and User Maual. Department of Mathematics, The University of Western Australia, Nedlands, WA 6907, Australia, 2004. Version 3. Available from: <http://www.cado.uwa.edu.au/miser/>.
[39] M.I. Kamien, N.L. Schwartz, Dynamic Optimization: The Calculus of Variations and Optimal Control in Economics and Management, Advanced Textbooks in Economics, second ed., vol. 31, North-Holland, 1991.
[40] D. Keil, R.W. Luebke, S.B. Pruett, Quantifying the relationship between multiple immunological parameters and host resistance: probing the limits of reductionism, J. Immunol. 167 (2001) 4543.
[41] Denise Kirschner, John Carl Panetta, Modeling immunotherapy of the tumor–immune interaction, J. Math. Biol. 37 (1998) 235.
[42] M. Kolev, Mathematical modelling of the competition between tumors and immune system considering the role of the antibodies, Math. Comput. Model. 37 (2003) 1143.
[43] Arthur J. Krener, The high order maximal principle and its application to singular extremals, SIAM J. Control Optim. 15 (2) (1977) 256.
[44] V. Kuznetsov, G.D. Knott, Modeling tumor regrowth and immunotherapy, Math. Comp. Model. 33 (2001) 1275.
[45] V. Kuznetsov, I. Makalkin, M. Taylor, A. Perelson, Nonlinear dynamics of immunogenic tumors: parameter estimation and global bifurcation analysis, Bull. Math. Bio. 56 (2) (1994) 295.
[46] V.A. Kuznetsov, G.D. Knott, Modeling tumor regrowth and immunotherapy, Math. Comput. Model. 33 (2001) 1275.
[47] Urszula Ledzewicz, Tim Brown, Heinz Schattler, Comparison of optimal controls for a model in cancer chemotherapy with l_1 and l_2 type objectives, Optim. Meth. Software 19 (3–4) (2004) 339.
[48] Urszula Ledzewicz, Heinz Schattler, Drug resistance in cancer chemotherapy as an optimal control problem, Discrete Contin. Dynam. Syst. Ser. B 6 (1) (2006) 129.

[49] U. Lucia, G. Maino, Thermodynamical analysis of the dynamics of tumor interaction with the host immune system, Physica A 313 (2002) 569, doi:10.1016/S0378-4371(02)00980-9.
[50] D.L. Lukes, Differential Equations: Classical to Controlled, vol. 162, Academic Press, 1982.
[51] Maplesoft. Maple. Version 9. Available from: <http://www.maplesoft.com/>.
[52] F.M. Marincola, E. Wang, M. Herlyn, B. Seliger, S. Ferrone, Tumors as elusive targets of T-cell-based active immunotherapy, Trends Immunol. 24 (2003) 335.
[53] The Mathworks. MATLAB. Version 7. Available from: <http://www.mathworks.com/>.
[54] Alexey Matveev, Andrey Savkin, Application of optimal control theory to analysis of cancer chemotherapy regimens, Syst. Control Lett. 46 (2002) 311.
[55] J.M. Murray, Some optimality control problems in cancer chemotherapy with a toxicity limit, Math. Biosci. 100 (1990) 49.
[56] F. Nani, H.I. Freedman, A mathematical model of cancer treatment by immunotherapy, Math. Biosci. 163 (2000) 159.
[57] M.R. Owen, J.A. Sherratt, Mathematical modelling of macrophage dynamics in tumours, Math. Mod. Meth. Appl. Sci. 9 (1999) 513.
[58] D.M. Pardoll, Cancer vaccines, Nat. Med. 4 (5) (1998) 525 (Vaccine Supplement).
[59] M.C. Perry (Ed.), The Chemotherapy Source Book, third ed., Lippincott Williams & Wilkins, 2001.
[60] L.S. Pontryagin, V.G. Boltyanskii, R.V. Gamkrelidze, E.F. Mishchenko, The Mathematical Theory of Optimal Processes, Gordon and Breach, 1962.
[61] S.A. Rosenberg, J.C. Yang, N.P. Restifo, Cancer immunotherapy: moving beyond current vaccines, Nat. Med. 10 (9) (2004) 909.
[62] A. Schwartz, E. Polak, Y. Chen, RIOTS: Recursive Integration Optimal Trajectory Solver. A Matlab Toolbox for Solving Optimal Control Problems, 1997. Version 1 for Windows. Available from: <http://www.schwartz-home.com/adam/RIOTS/>.
[63] R.A. Sharma, A.G. Dalgleish, W.P. Steward, K.J. O'Byrne, Angiogenesis and the immune response as targets for the prevention and treatment of colorectal cancer (review), Oncol. Rep. 10 (2003) 1625.
[64] O. Sotolongo-Costa, L.M. Molina, D.R. Perez, J.C. Antoranz, M.C. Reyes, Behavior of tumors under nonstationary therapy, Physica D 178 (2003) 242, doi:10.1016/S0167-2789(03)00005-8.
[65] R.F. Stengel, R. Ghigliazza, N. Kulkarni, O. Laplace, Optimal control of innate immune response, Optim. Control Appl. Meth. 23 (2002) 91.
[66] Andrzej Swierniak, Urszula Ledzewicz, Heinz Schattler, Optimal control for a class of compartmental models in cancer chemotherapy, Int. J. Appl. Math. Comput. Sci. 13 (3) (2003) 357.
[67] Zuzanna Szymanska, Analysis of immunotherapy models in the context of cancer dynamics, Int. J. Appl. Math. Comput. Sci. 13 (3) (2003) 407.
[68] T. Takayanagi, A. Ohuchi, A mathematical analysis of the interactions between immunogenic tumor cells and cytotoxic T lymphocytes, Microbiol. Immunol. 45 (2001) 709.
[69] O. von Stryk, Numerical solution of constrained optimal control problems by DIRect COLlocation. Lehrstuhl M2 Numerische Mathematik, Technische Universitaet Muenchen, 1999. Version 2.1. Available from: <http://www.sim.informatik.tu-darmstadt.de/sw/dircol/dircol.html>.
[70] R. Wallace, D. Wallace, R.G. Wallace, Toward cultural oncology: The evolutionary information dynamics of cancer, Open Syst. Inf. Dyn. 10 (2003) 159.
[71] S.D. Webb, J.A. Sherratt, R.G. Fish, Cells behaving badly: a theoretical model for the Fas/FasL system in tumour immunology, Math. Biosci. 179 (2002) 113.
[72] L.M. Wein, J.T. Wu, D.H. Kirn, Validation and analysis of a mathematical model of a replication-competent oncolytic virus for cancer treatment: implications for virus design and delivery, Cancer Res. 63 (2003) 1317.
[73] C.J. Wheeler, D. Asha, L. Gentao, J.S. Yu, K.L. Black, Clinical responsiveness of glioblastoma multiforme to chemotherapy after vaccination, Clin. Cancer Res. 10 (2004) 5316.
[74] D. Wodarz, Viruses as antitumor weapons: Defining conditions for tumor remission, Cancer Res. 61 (2001) 3501.
[75] D. Wodarz, V.A.A. Jansen, A dynamical perspective of ctl cross-priming and regulation: implications for cancer immunology, Immunol. Lett. 86 (2003) 213.